



Fire parameterization on a global scale

O. Pechony¹ and D. T. Shindell¹

Received 17 February 2009; revised 22 April 2009; accepted 12 June 2009; published 29 August 2009.

[1] We present a convenient physically based global-scale fire parameterization algorithm for global climate models. We indicate environmental conditions favorable for fire occurrence based on calculation of the vapor pressure deficit as a function of location and time. Two ignition models are used. One assumes ubiquitous ignition, the other incorporates natural and anthropogenic sources, as well as anthropogenic fire suppression. Evaluation of the method using Global Precipitation Climatology Project precipitation, National Centers for Environmental Prediction/National Center for Atmospheric Research temperature and relative humidity, and Moderate Resolution Imaging Spectroradiometer (MODIS) Leaf Area Index as a proxy for global vegetation density gives results in remarkable correspondence with global fire patterns observed from the MODIS and Visible and Infrared Scanner satellite instruments. The parameterized fires successfully reproduce the spatial distribution of global fires as well as the seasonal variability. The interannual variability of global fire activity derived from the 20-year advanced very high resolution radiometer record are well reproduced using Goddard Institute for Space Studies general circulation models climate simulations, as is the response to the climate changes following the eruptions of El Chichon and Mount Pinatubo. In conjunction with climate models and data sets on vegetation changes with time, the suggested fire parameterization offers the possibility to estimate relative variations of global fire activity for past and future climates.

Citation: Pechony, O., and D. T. Shindell (2009), Fire parameterization on a global scale, *J. Geophys. Res.*, 114, D16115, doi:10.1029/2009JD011927.

1. Introduction

[2] Wildland fires are a global scale environmental process, with a profound impact on global climate and air quality through emissions of greenhouse gases and aerosols (and their precursors), and impact on vegetation. Conversely, changes in climate have the potential to significantly affect fire regimes. The link between fires and climate raises the need to incorporate this important parameter in climate models. To represent fire occurrence on a global scale, two general approaches are possible [Flannigan *et al.*, 2005a, 2005b]. One is to incorporate a suite of fire models, each developed for a specific ecosystem. This approach seems to be not practical for long-term global fire modeling, since with change of climate, ecosystems for which the specific fire model was developed and calibrated may change and require new calibration, or even use of an alternative fire model. Another approach, which we incorporate here, is to develop a simpler, more general model for all ecozones, which does not require local calibration. Simple generalized models omit many fine details (3D fuel distribution, different ignitability of fuels, etc.), which are important for predicting fire behavior on

small scales. However, on a global scale these details may introduce increasing uncertainty, as many of these parameters are hard, or even impossible to quantify globally. A simple model gives generalized results. But the principles of a simple model hold globally and through time.

[3] A few models have been suggested to characterize global fire occurrence. The fire model in the Lund-Potsdam-Jena (LPJ) Dynamic Global Vegetation Model (DGVM) [Thonicke *et al.*, 2001] estimates fire activity based on topsoil layer moisture content and dead fuel amount. The fire module of the Canadian Terrestrial Ecosystem Model (CTEM) DGVM [Arora and Boer, 2005] estimates the probability of fire occurrence depending on fuel availability and fuel moisture, and presence of an ignition source (anthropogenic or natural). These models have been validated only for a handful of locations, however, and substantial work will certainly be required to use them effectively on a global scale in general circulation models (GCMs). Venevsky *et al.* [2002] suggested a model that uses the Nesterov fire danger index, which relies on the dew-point deficit and precipitation, to estimate the number of fires in a region. The Nesterov index is functional only at above-zero temperatures, thus limiting the applicability of the model both in space and time. There is therefore a need for a global fire model that is specifically designed for a global use, and validated on a global scale against satellite records which are the only source of consistent information on fires on a global scale [Chuveico *et al.*, 2008].

¹NASA Goddard Institute for Space Studies, Columbia University, New York, New York, USA.

[4] Here we suggest a simple global fire algorithm for use with GCMs. Realizing the enormous complexity of fire as a physical process that depends on myriad parameters, it is neither practical, nor possible to account for all details when modeling global fires at coarse resolutions. In such a case, it is reasonable to concentrate on the most important factors that define fire occurrence, while also keeping in mind the availability of reliable global information on these factors. The model we suggest determines worldwide flammability conditions from vegetation density and a set of meteorological parameters: precipitation, relative humidity, and temperature. These parameters are readily available, and are well verified on a global scale. Given a distribution of ignition sources, the algorithm provides the global distribution of fire counts, which can be verified against actual satellite multi-year records, readily available from a number of different sensors. We explore two ignition source distributions. One assumes a ubiquitous ignition source. The other incorporates both natural and anthropogenic sources, as well as anthropogenic fire suppression. The suggested procedure leads to a good representation of fire occurrence on a global scale, and can be used with climate models to examine the relative changes in past and future global fires, and aid in estimation of past and future trends in fire emissions.

2. Flammability Estimation

[5] There are several flammability meters, or fire-danger indices, that are in use today. These include the Keetch-Byram drought index [Keetch and Byram, 1968], the Canadian forest fire weather index [Van Wagner, 1987], the Nesterov Index [Nesterov, 1949] and the McArthur fire-danger (meter) index, quantified by Noble *et al.* [1980]. These rating systems were developed and calibrated for specific geographical areas, and require calibration and/or modification to be applied elsewhere. The Zhdanko flammability index [Zhdanko, 1965] and the Modified Nesterov index [Nesterov, 1949] (both show similar performance [Groisman *et al.*, 2007]) are based on evaluation of the humidity deficit from the dew-point deficit and rainfall, represented by empirically derived discrete rain coefficients that exhibit exponential increase with rain rate. Both indices are only functional at above-zero temperatures.

[6] In our model we have incorporated the vapor pressure deficit, VPD as an indicator of flammability conditions. VPD is one of the most important drivers of the evaporation rate [Anderson, 1939; Castellvi *et al.*, 1996; Saugier *et al.*, 1997], and it can be fairly easily calculated from relative humidity, RH (in %), and temperature, T (in °K). In terms of the saturation vapor pressure e_s and the actual vapor pressure e , VPD is expressed as $VPD = (e_s - e)$, and can be rewritten as $VPD = e_s (1 - RH/100)$. The saturation vapor pressure e_s can be calculated from the Goff-Gratch equation [Goff and Gratch, 1946; Goff, 1957]: $e_s = e_{st} 10^{Z(T)}$, where $e_{st} = 1013.246$ [mb] (saturation vapor pressure at water boiling point) and

$$Z(T) = a \left(\frac{T_s}{T} - 1 \right) + b \cdot \log \left(\frac{T_s}{T} \right) + c \left(10^{d \left(\frac{T_s}{T} - 1 \right)} - 1 \right) + f \left(10^{h \left(\frac{T_s}{T} - 1 \right)} - 1 \right) \quad (1)$$

The constants are [Goff and Gratch, 1946]: $a = -7.90298$; $b = 5.02808$; $c = -1.3816 \cdot 10^{-7}$; $d = 11.344$; $f = 8.1328 \cdot 10^{-3}$; $h = -3.49149$; and $T_s = 373.16$ (°K) (water boiling point temperature). Thus:

$$VPD \propto 10^{Z(T)} (1 - RH/100) \quad (2)$$

We assume an inverse exponential dependence of flammability on precipitation, of the form $\exp(-c_R R)$ (following Keetch and Byram [1968], and instead of the discrete rain coefficient used in the Zhdanko and Nesterov indices). Here R is the surface rain rate in mm/day and $c_R = 2$ (day/mm).

[7] Further, we introduce a vegetation density coefficient VD , which ranges from 0 for no vegetation and to 1 for dense vegetation. Note that VD is not a measure of vegetation flammability, but is solely a measure of density of vegetation of any kind and condition. Whether this vegetation is dry or moist is determined by physical factors affecting the vegetation.

[8] We can then write the flammability F at time step t and grid cell (i, j) as:

$$F(t)_{ij} = 10^{Z(T(t)_{ij})} \left(1 - \frac{RH(t)_{ij}}{100} \right) VD(t)_{ij} \exp(-c_R R(t)_{ij}) \quad (3)$$

In this work we employ a monthly time step, which is a reasonable timescale for representing the response of fires to climate conditions. When using this method for finer time steps (days, hours) one would have to use appropriate time-averaged precipitation values to avoid unrealistically high flammability fluctuations in time steps with isolated events of very low, or zero, precipitation.

[9] We thus derive the flammability, a parameter which indicates conditions favorable for fire occurrence. Although this simple model cannot compete with local fine-scale fine-tuned fire models in predicting small-scale features of regional fire activity, this is not the aim. Looking at climate change as a long-term global process, small-scale temporal and spatial variations lose much of their importance, thus the objective is to reproduce the general large-scale spatial and temporal patterns of global fire occurrence.

3. Ignition Sources

[10] Whether or not the fire will actually occur in given conditions depends on the availability of an ignition source (either anthropogenic or natural). There are two main sources of ignition: lightning discharges and human activities. Humans influence fire patterns not only by adding ignition sources, but also by suppressing both anthropogenic and natural fires. Both effects increase with increasing population, to some extent canceling each other. We test two ignition source models. One incorporates anthropogenic and lightning ignitions, and anthropogenic fire suppression. The other assumes a ubiquitous ignition source.

3.1. Lightning Activity

[11] Up-to-date, lightning data collected by the Optical Transient Detector (OTD) satellite-based sensor [Christian *et al.*, 1996], remains the only available record of global lightning flash rate. OTD supplies the total flash rate: both intracloud (IC), and cloud-to-ground (CG) flashes.

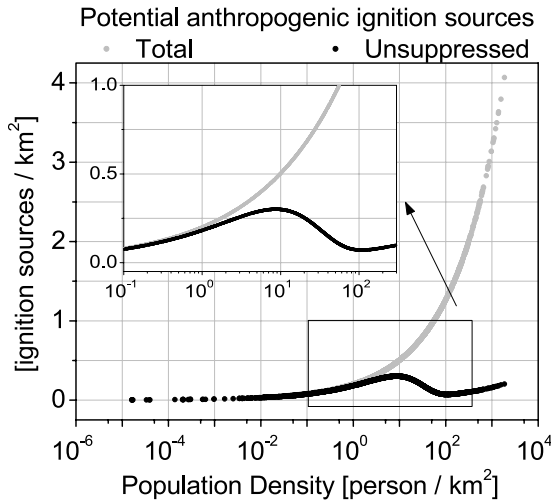


Figure 1. Number of potential anthropogenic ignition sources per km^2 per month as a function of population density. The plot shows both total number of anthropogenic sources (gray), and those that will potentially remain unsuppressed (black).

Obviously, only CG flashes can ignite a fire. *Prentice and Mackerras* [1977] proposed the following widely used relation between the ratio of IC to CG flashes z , and latitude λ :

$$z = 4.16 + 2.16 \cos(3\lambda) \quad (4)$$

Using this relation, an estimate of the number of CG flashes can be obtained from OTD records. We use these as a number of natural ignition sources, I_N .

3.2. Anthropogenic Influence

[12] Most studies modeling anthropogenic ignitions are dealing with small local scales [e.g., *Martell et al.*, 1989; *Guyette et al.*, 2002; *Martinez et al.*, 2008]. An exception is the study by *Venevsky et al.* [2002], who utilizes the relation between number of anthropogenic ignitions and population density, suggested by *Telitsyn* [1988] for assessment of human ignitions in Khabarovskiy Krai, Russia. *Venevsky et al.* [2002] test the procedure for Peninsular Spain, but it is suggested to be applicable globally. Following *Venevsky et al.* [2002], the number of anthropogenic ignition sources per km^2 per month, I_A is expressed as:

$$I_A = k(PD)PD^\alpha \quad (5)$$

Where PD is the population density; $k(PD) = 6.8PD^{-0.6}$ is a function representing different ignition potentials of humans in areas with different population densities (assuming that people living in scarcely populated regions interact more with natural ecosystems, and therefore produce potentially more ignitions); $\alpha = 0.03$ (ignition sources per person per month per km^2) is the number of potential ignition sources (not the number of “successful” ignitions, which depends on flammability) produced by one human per unit time. Such an approach allows the introduction of anthropogenic ignition sources with respect to population density, but will not depict intentional burning, such as seasonal land

clearing, or deforestation fires. Given that appropriate data is available, the approach can be made more sophisticated by allowing α and k to vary in space and time.

[13] Humans actively suppress both anthropogenic and natural fires. Firefighting policies and their effectiveness depend on cultural, economical, and other factors. In general, success of fire suppression depends on early fire detection. We assume that in highly populated areas fires are detected earlier and suppressed more effectively than in scarcely populated areas, and the fraction of suppressed fires increases with increasing population density. Assuming exponential dependence, we can formulate the fraction of nonsuppressed fires, f_{NS} as:

$$f_{NS} = c_1 + c_2 \exp(-\omega PD) \quad (6)$$

The fraction of fires that remain unsuppressed at the most populated areas is expressed by c_1 . The maximum number of fires that remain unsuppressed at the distant, unpopulated regions is defined by the sum of c_1 and c_2 , and the rate at which the number of unsuppressed fires decreases with increasing population density is determined by ω . Owing to the lack of global quantitative data, constant values are selected in a rather heuristic manner: $c_1 = 0.05$, $c_2 = 0.9$, $\omega = 0.05$. Thus, up to 95% of fires are assumed to be suppressed in the densely populated regions, and 95% are assumed to remain unsuppressed in unpopulated regions. When appropriate global data becomes available, these constants can be determined more accurately and can also vary across the globe, and with time to reflect different fire suppression capabilities in different socio-economic conditions.

[14] Figure 1 illustrates the effect of fire suppression (as defined in equation (6)) on the number of potential anthropogenic sources (defined in equation (5)). Fire suppression starts to take effect, decreasing the number of potential ignition sources, at densities of ~ 1 person/ km^2 , and above. The number of unsuppressed ignition sources, $f_{NS}I_A$, peaks at population density of ~ 10 person/ km^2 , and then falls, due to increased fire suppression. At population densities over ~ 100 person/ km^2 the number of unsuppressed sources starts to rise again. This behavior is conditioned by the assumption of a maximum 95% fire suppression rate, which is quite uncertain. However, in places with such dense population, there is limited fuel availability. Thus, despite the increasing number of ignition sources, the actual number of fires will still be low.

[15] The number of fires (fire counts) in a time step per km^2 , N_{fire} is determined as a product of flammability F , the sum of anthropogenic and natural ignition sources, and the fraction of unsuppressed fires:

$$N_{fire} = F(I_N + I_A)f_{NS} \quad (7)$$

In the ubiquitous model, the number of sources is constant, and there is no fire suppression.

4. Input and Reference Data

[16] The following input parameters are used in the model: precipitation, temperature, relative humidity, vegetation density, population density and lightning flash rate, derived from monthly climatology OTD data.

[17] We used precipitation data from the Global Precipitation Climatology Project (GPCP) version 2 monthly $2.5^\circ \times 2.5^\circ$ resolution merged satellite and rain gauge data set [Adler *et al.*, 2003], distributed by National Climatic Data Center (NCDC). The GPCP version 2 data combines precipitation estimates from Special Sensor Microwave Imager (SSM/I) emission and scattering algorithms, GOES Precipitation Index (GPI), Outgoing longwave Precipitation Index (OPI), rain gauges, and TOVS sounders on NOAA polar orbiting satellites.

[18] Temperature and relative humidity monthly data at $2.5^\circ \times 2.5^\circ$ resolution was obtained from the National Centers for Environmental Prediction (NCEP)/National Center for Atmospheric Research (NCAR) reanalysis [Kalnay *et al.*, 1996].

[19] Population density was obtained from the Gridded Population of the World Version 3 (GPWv3) [CIESIN, 2005].

[20] As a proxy for vegetation density we have used annual mean normalized (by its maximum) Leaf Area Index (LAI) derived from the Moderate Resolution Imaging Spectroradiometer (MODIS) Terra MOD15A2 product [Garrigues *et al.*, 2008]. The original $0.25^\circ \times 0.25^\circ$ resolution was downscaled to $2.5^\circ \times 2.5^\circ$ to match the resolution of the GPCP and NCEP/NCAR data. LAI gives an estimate of the total green leaf area, and its annual variations reflect the varying greenness of the vegetation in the area: dry grass and foliage produce low LAI values. In our model vegetation density reflects only the amount of potential fuel; its state (dry or moist) is determined by ambient conditions. We therefore averaged LAI values to obtain an approximate representation of the global vegetation density. Note that to account for changes in vegetation density with time, the fire model can be coupled to a DGVM or use vegetation density data either from a DGVM or derived from land use change data sets such as those used as boundary conditions in many climate models that do not contain DGVMs (e.g., as in the IPCC AR4 simulations) or in many paleoclimate studies.

[21] As reference data we used MODIS/Terra monthly $1^\circ \times 1^\circ$ resolution Active Fire Product V004 (MOD14CM1) published by NASA NEESPI Data and Service Center [Leptoukh *et al.*, 2007]. MODIS data has global coverage. In addition we used the Tropical Rainfall Measuring Mission (TRMM) Visible and Infrared Scanner (VIRS) $0.5^\circ \times 0.5^\circ$ resolution monthly fire product [Giglio *et al.*, 2003]. VIRS data set coverage is between 40N and 40S latitudes. Both data sets were downscaled from the original resolution to $2.5^\circ \times 2.5^\circ$ to match the resolution of the input data sets. We also examined fire data from the Along Track Scanning Radiometer (ATSR), but found it to differ strongly from the other two sensors, especially in the northern latitudes. This is in general agreement with results published by Kasischke *et al.* [2003], who showed that ATSR data do not represent an unbiased sample of fire activity, and its monitoring scheme does not seem to be effective at higher latitudes. Hence, we use only MODIS and VIRS data for evaluation. The satellite records provide fire counts as the number of recorded fire events in a pixel. As such, persistent fires can be counted more than once, and short-tem fires may be omitted. Nevertheless, at present, satellite fire count records are the

most consistent and reliable proxy of global fire occurrence [e.g., Chuveico *et al.*, 2008; Giglio *et al.*, 2006].

[22] Calculations presented below were performed for the years 2001–2005, the years for which data from all sensors overlap. Over this short period, vegetation density was considered constant. We parameterized fires on a monthly basis, with $2.5^\circ \times 2.5^\circ$ resolution (the resolution of the input data). Then, annual and seasonal averages were calculated for years 2001–2005.

5. Results

[23] Figure 2 shows MODIS and modeled 2001–2005 annual mean fire counts as a function of population density. Model results are shown for three source distributions: ubiquitous, lightning-only, and lightning and anthropogenic. The inserts on each plot show the mean fire count as a function of population density. MODIS fire counts increase with increasing population, peak at 10–20 (persons/km²), and then decrease. Lightning fires show small values for all population densities. Ubiquitous ignition model reasonably reproduces MODIS fire behavior, showing increase in fire counts toward 10–20 (person/km²) but the peak is less pronounced. Introducing anthropogenic effect further improves the correspondence. The peak is more pronounced than in the ubiquitous ignition model, closer to MODIS records. The following decrease of fires with population is also sharper than in the ubiquitous ignition model, closer to MODIS records. The model produces on average about 10 times more human-caused than lightning-caused fires, corresponding to the range of anticipated values [e.g., Price, 1994; Wotton *et al.*, 2003; Martinez *et al.*, 2008].

[24] The spatial distribution of the 2001–2005 annual mean fires is shown in Figure 3. Satellite estimates provide information on fire patterns, but the values of fire counts differ strongly between different instruments, therefore the results are presented in normalized (to their maxima) fire counts. Both models reproduce the major patterns of global fire activity in good agreement with distributions observed by MODIS and VIRS sensors. India and Myanmar (Burma) are clearly overestimated in the ubiquitous model, but are well reproduced when anthropogenic effect is accounted for. India and southeastern Myanmar are two of the world's most densely populated areas, where most vegetation is actively managed by humans (crop production maps in the work of Foley *et al.* [2007]). The ubiquitous model that does not account for anthropogenic effects cannot depict the fire activity in a region with such overwhelming human influence. Taking into account fire suppression allows the model to properly reflect the level of fire activity in this area. Representation in other regions does not appear to be notably affected by accounting for anthropogenic influence.

[25] The scatterplot in Figure 4 shows parameterized fires and VIRS records plotted as a function of collocated MODIS fire counts. This plot allows quantitative estimation of the model performance. The correlation between the modeled and MODIS fires is $r = 0.71$ for ubiquitous source model and $r = 0.74$ for model incorporating anthropogenic effects. This is comparable to the correlation between the two recorded data sets, MODIS and VIRS, which is $r = 0.77$.

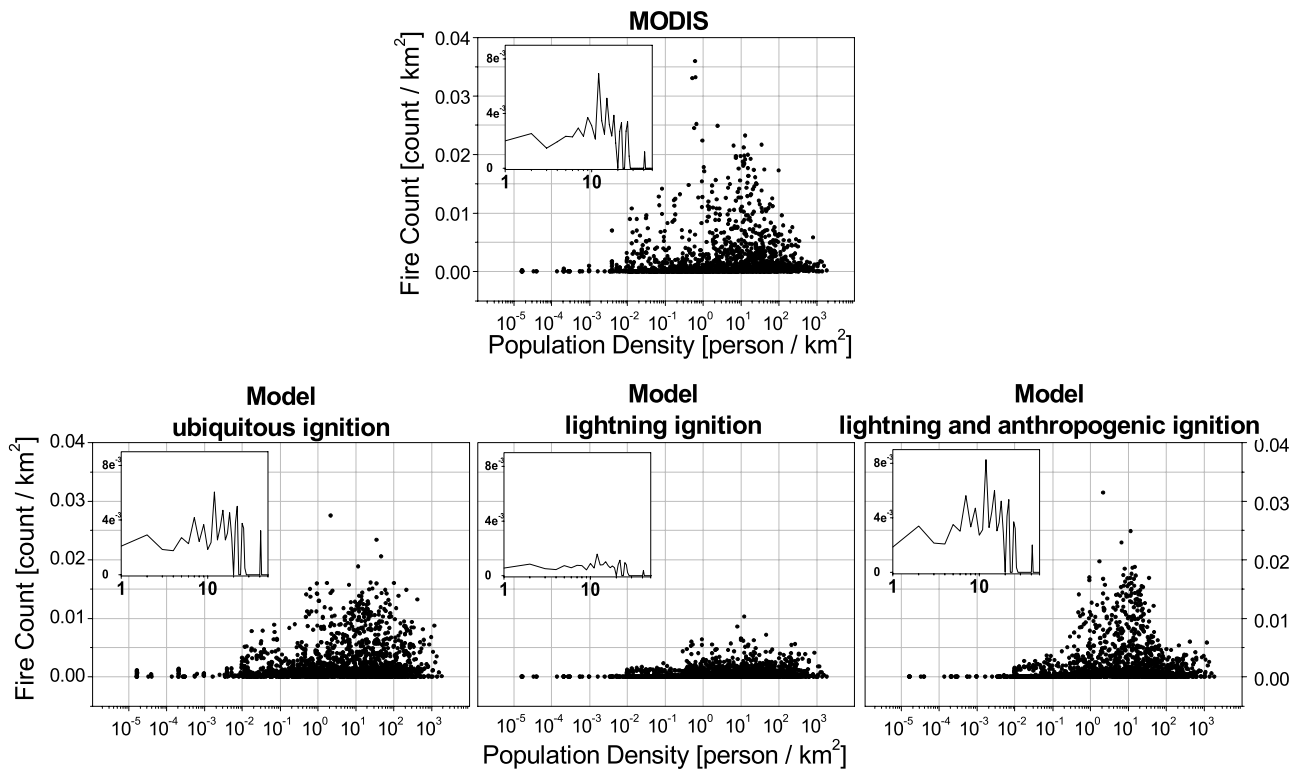


Figure 2. The 2001–2005 annual mean fire counts as a function of population density: MODIS and modeled with ubiquitous source, lightning sources and lightning and anthropogenic sources.

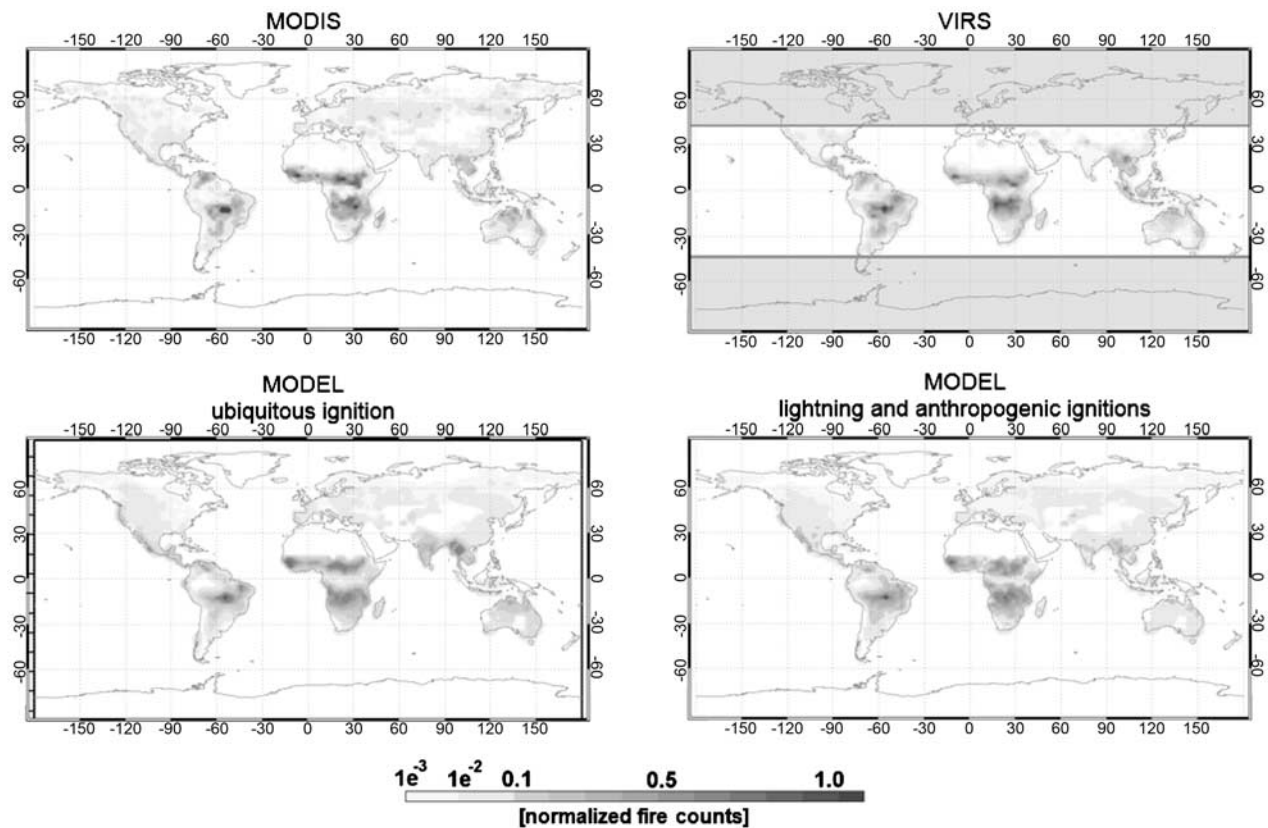


Figure 3. The 2001–2005 annual mean fires recorded by MODIS and VIRS, and model parameterization with ubiquitous and lightning and anthropogenic ignition sources.

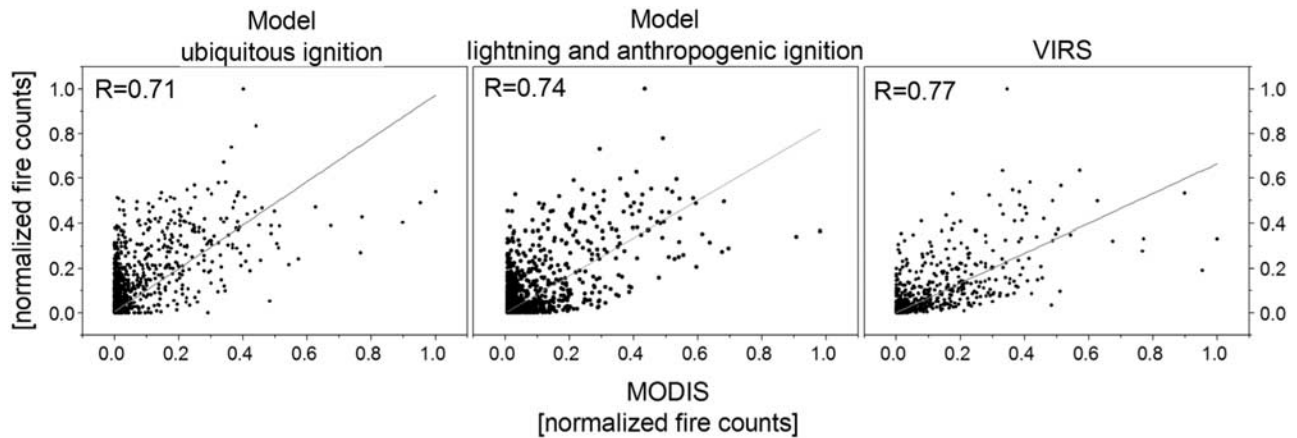


Figure 4. Scatterplot of 2001–2005 annual mean fire counts in collocated grid boxes: model parameterization with ubiquitous, lightning and anthropogenic ignition sources, and VIRS records versus MODIS records. Solid lines show least squares linear fit.

[26] Figure 5 shows the zonal average fire counts. Both ubiquitous and anthropogenic plus lightning source models reproduce the distribution of global fire activity with latitude reasonably well. The plot clearly illustrates fires in India and Myanmar that are overestimated in ubiquitous model, but are “corrected” by including anthropogenic effect. Another region that deviates from both sensors is the sub-Sahara Sahel. Here both models reproduce the general picture very well, but the parameterized fires do not drop off moving northward as rapidly as in the satellite observations. This could be due to several reasons. Slightly wider Sahara borders than depicted by LAI data would be sufficient to produce this effect. In addition, this region is one of the most intensively used for agriculture (crop production maps in the work of *Foley et al.* [2007]), and the fire regimes are, to a large extent, defined by local agricultural habits. Fires in Siberia are underestimated by both models, comparing to MODIS records (VIRS observations do not extend this far north). Siberia, one of the least populated places on Earth, experienced a great increase in the number of fires over the past years [*Soja et al.*, 2007]. This was initially suggested to be a manifestation of climate change in the region [*Dale et al.*, 2001; *Schiermeier*, 2005]. However, further analysis indicated that a vast part of this increase is directly induced by human activity [*Mollicone et al.*, 2006]. The human impact on fires significantly in-

creased in the post-Soviet period owing to lack of control, new socioeconomic conditions and the Siberia oil boom [*Dienes*, 2004]. During the years 2002–2005, the density of fire events in Siberia regions subject to intense human influence was an order of magnitude higher than in the neighboring regions of intact forest [*Mollicone et al.*, 2006]. This suggests that majority of Siberian fires are directly related to anthropogenic activity, conditioned by extraordinary socio-economic factors, and not by climatic conditions, or population densities. As such, these fires cannot be depicted by the ubiquitous model, or by introducing population density-dependent anthropogenic effects. Overall both models show high correlation coefficients of 0.80–0.89 with MODIS and VIRS records (summarized in Figure 5) which is comparable to the correlation between the two recorded data sets, MODIS and VIRS ($r = 0.87$). Examination of correlations for individual continents (Table 1) demonstrates that in most cases the anthropogenic model improves correspondence with one of the sensors, while decreasing correspondence with the other. In North America the ubiquitous model shows significantly better correspondence with both sensors. This could be due to fire management policies that should be reflected with a different set of coefficients for equations (5) and (6). The relative contribution of each continent to global fires is well depicted by both models (Figure 6).

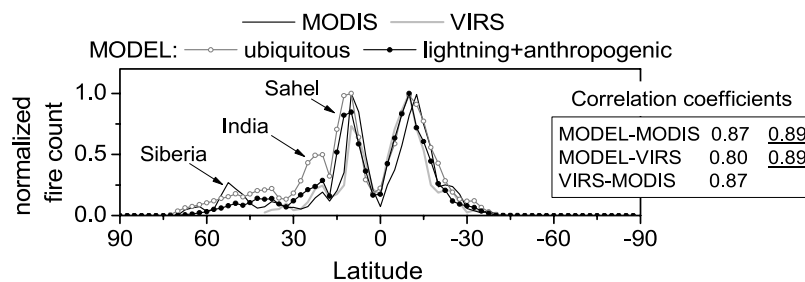


Figure 5. The 2001–2005 annual mean zonal average fires recorded by MODIS and VIRS, and model parameterization with ubiquitous and lightning plus anthropogenic ignition sources. Correlation coefficients are summarized on the plot (correlation coefficients for model with anthropogenic effect are underlined).

Table 1. Annual Correlation Coefficients for Individual Continents^a

	Measurements	Ubiquitous Model	Anthropogenic Model
Africa	0.94	0.84 <i>0.77</i>	0.75 <i>0.83</i>
Australia	0.97	0.94 <i>0.93</i>	0.82 <i>0.89</i>
South America	0.86	0.86 <i>0.99</i>	0.87 <i>0.97</i>
North America*	0.85	0.87 <i>0.86</i>	0.62 <i>0.74</i>
Eurasia*	0.87	0.68 <i>0.90</i>	0.72 <i>0.86</i>

^aBetween MODIS and VIRS measurements, model and MODIS (regular font), and model and VIRS (italic font). Asterisks indicate that VIRS coverage in North America and Eurasia is partial.

[27] Seasonal latitudinal drift of dominant fires is equally well reproduced with both models, though correlations with observations are slightly larger in winter and fall with the anthropogenic and lightning source model (Figure 7). Both seasonal variations and the relative magnitude of fires are well depicted (the values are normalized to the maximal value of the four seasons). The model underestimates the magnitude of September–October–November burning in South America, which is largely intentional burning for land clearing during this season (and as such cannot be depicted by ubiquitous model or by introducing effects depending on population density). The correlation between the parameterized and observed fires is high for all seasons (summarized in Figure 7), with lower correlations in March–April–May, the season with lowest global fire activity, and the least pronounced fire pattern.

[28] The changes between ubiquitous and anthropogenic plus lightning models are not significant, in some regions improving correspondence with one of the sensors, while decreasing correspondence with the other. Fires modeled with ubiquitous ignition source are not related to population density, or lightning distribution, and only reflect the flammability conditions. Their similarity to satellite fire records suggests that on a global scale fire distribution is determined predominantly by flammability conditions (which eventually define both success of ignition and effectiveness of fire suppression). Spatial variations in source abundance are, to some extent, canceled out by differences in effectiveness of fire suppression.

6. Interannual Variations

[29] There are few long-term records of global fire activity. The most long-term estimates are offered by *Mouillot and Field* [2005] reconstruction, which combines perhaps all possible sources of information on past century fires. Being an excellent source of reference on records of historical fires worldwide, other use of data presented in that work should be made with caution. The estimates are based on scattered, mostly qualitative, and often contradictory, records, and disregarding climate variations. Another relatively long-term data set is the AVHRR-derived burnt area estimates for 1982–2000 [*Riano et al.*, 2007]. Though these estimates do not provide meaningful absolute values, they do supply useful information on temporal trends [*Riano et al.*, 2007; D. Riano, personal communication]. We therefore exploit the 20-year AVHRR burnt area record to evaluate interannual variability and response to volcanic-induced climate change in the model results.

[30] We estimate burnt areas from modeled fire counts, incorporating the *Van der Werf et al.* [2003] approach. Burned area, BA , is assumed to be proportional to fire counts, FC , as $BA = wFC$, when w is a function representing the dependence of effective burned area per fire count on vegetation density, giving more weight to fire counts detected in sparsely vegetated areas, where fires spread rapidly, and the effective burnt area per fire count is the largest. As a proxy of global burnt area we used the 2001–2005 Global Fire Emissions Database (GFED) inventory burned area product [*Van der Werf et al.*, 2006]. We derived the function w , as a mean ratio of 2001–2005 annual mean MODIS fire counts and the GFED burned areas, as a function of vegetation density (Figure 8), and applied it to the modeled fire counts.

[31] Figure 9 shows interannual variations of global burned area from the GFED inventory, based on the MODIS fire and burned area data [*Van der Werf et al.*, 2006], L3JRC estimates, based on the SPOT VEGETATION reflectance data [*Tansey et al.*, 2007], and ubiquitous ignition model results. Note, that not a calendar year, but a fire year (April–March) is considered, to allow consistent comparison with the L3JRC record. The correspondence between modeled and GFED burned area is quite good, though modeled values vary slightly less than GFED estimates. Both GFED and model estimates are markedly different from the L3JRC record. These results should be treated with caution. On a short time period of 4 years, no clear trend can be identified that could be caused by climate variations, and therefore should be reproduced by our model. Furthermore, the interannual variations of global burnt area are relatively small: at most $\sim 8\%$ deviation from the mean for GFED estimates and slightly higher, $\sim 12\%$ variations for L3JRC. Given uncertainties associated with burnt area estimates, these variations are highly tentative. It can be roughly said, that over this short period both GFED and L3JRC, and the model, show rather small interannual variations in global burnt areas.

[32] For comparison with the AVHRR record we used the ubiquitous ignition model with meteorology from GISS GCM historical climate simulations [*Hansen et al.*, 2007]. Following the desert definition of *Tucker et al.* [1991]

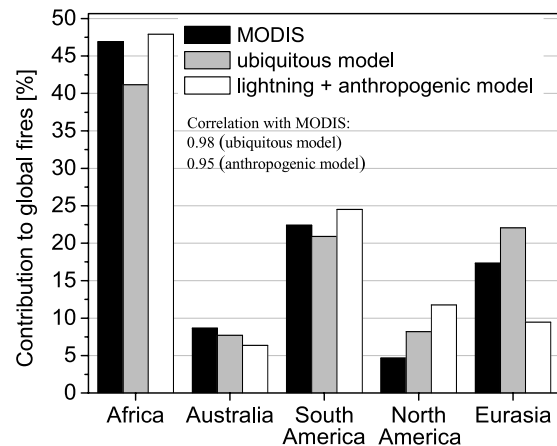


Figure 6. Relative contributions of individual continents to 2001–2005 annual mean global fire activity: MODIS measurements and model simulations.

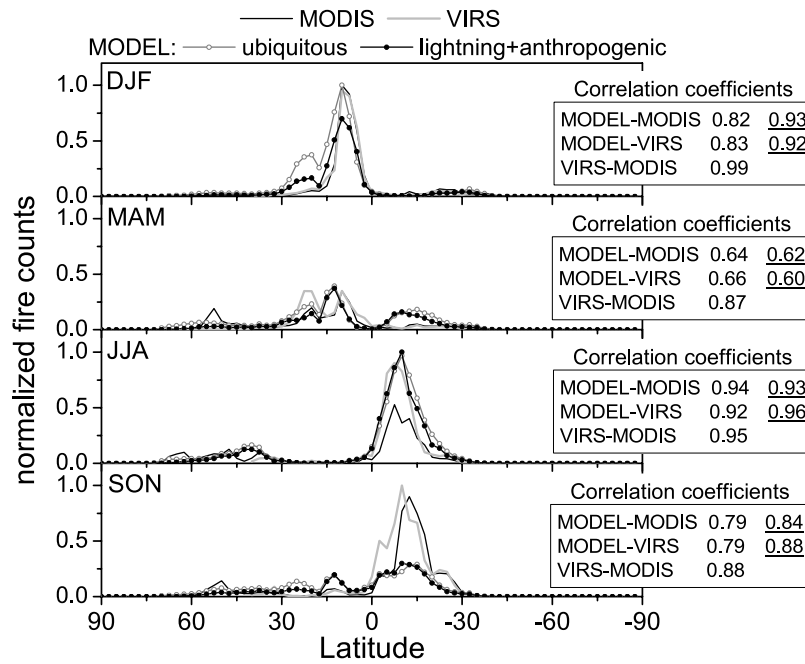


Figure 7. The 2001–2005 seasonal mean zonal average fires recorded by MODIS and VIRS, and model parameterization (ubiquitous and anthropogenic). Correlation coefficients are summarized on the plot (correlation coefficients for model with anthropogenic effect are underlined).

vegetation density was set to zero when annual precipitation was less than 200 mm/a, to avoid overestimating burning in regions that may have been arid in the past. The min-max difference in AVHRR burnt areas exceeds by far the variations seen in L3JRC and GFED estimates. For both AVHRR and model data we have subtracted the mean value and normalized each data set to their min-max difference to examine relative variations around the mean. The results are shown in Figure 10 (AVHRR data is partially missing for the years 1994 and 2000). The model reproduces the interannual variations reasonably well. It also depicts a slow increase of global fire activity, of which there is a suggestion in the AVHRR records as well. The model also reproduces the large deviations that follow the eruptions

of El Chichon and Pinatubo volcanoes. Large volcanic eruptions are included as climate forcings in the past climate simulations [Hansen et al., 2007]. They produce large temperature changes (global mean annual average decreases, seasonal increases in some continental interiors), as well as some precipitation reduction and shifts, thus influencing global fires. The model appears to capture the observed responses reasonably well, providing an important observation-based validation of the model’s sensitivity to climate change.

7. Summary

[33] In this work we present a simple procedure that allows global-scale fire parameterization based on four

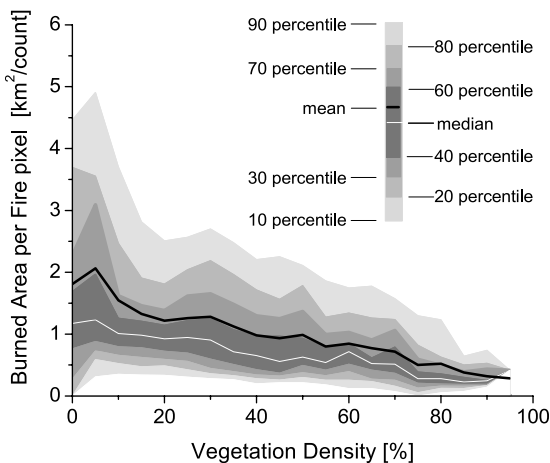


Figure 8. Burned area per fire pixel as a function of vegetation density (derived from 2001 to 2005 GFED burned area and MODIS fire counts).

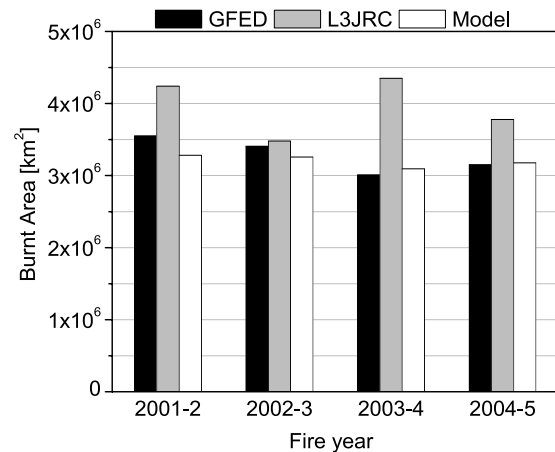


Figure 9. Interannual variations of global burned area (April–March): GFED and L3JRC estimates, and model results.

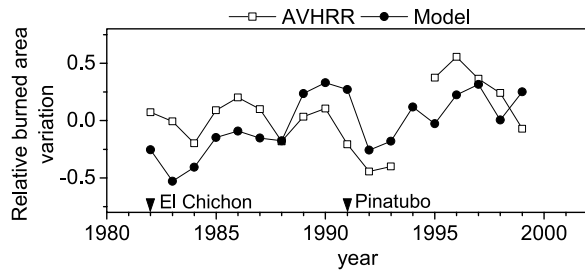


Figure 10. Relative variations around mean of global burnt area during 1982–2000: AVHRR estimates, and model simulation using GISS GCM climate fields.

physical parameters: precipitation, relative humidity, temperature, and vegetation density. Two models are tested: one with ubiquitous source and the other including lightning sources and anthropogenic influence. The anthropogenic effect includes both ignition and suppression of fires by humans, as a function of population density.

[34] Using GPCP precipitation, NCEP/NCAR relative humidity and temperature, and MODIS LAI as a proxy for global vegetation density we have modeled 2001–2005 fire activity. Both ubiquitous and anthropogenic models show good correspondence in large-scale fires with MODIS and VIRS records, reproducing both the global fire patterns and their seasonal variations quite well. Correlations between modeled and measured fires are in most cases comparable with correlation between the MODIS and VIRS data sets. Introducing anthropogenic influence significantly improves correspondence between model and measurements in densely populated regions. Otherwise, the changes are insignificant, often improving correspondence with one of the sensors, while decreasing correspondence with the other. The similarity between fires modeled in the ubiquitous ignition source model and satellite records suggests that distribution of global fire activity patterns are governed primarily by flammability variations. Differences in availability of sources are to some extent canceled out by differences in fire suppression effectiveness.

[35] Adequate representation of anthropogenic influences requires not only information on population densities, but also comprehensive global socio-economic data on sources of anthropogenic ignitions, fire suppression policies and resources, and degrees of fire management. This information is also necessary to estimate anthropogenic influence in past and future simulations. At present, however, such information is unavailable [Chuveico *et al.*, 2008]. Hence it is fortuitous that flammability variations alone play such an important role in global-scale fires. Nevertheless, large changes in population density, as well as significant changes in socio-economic conditions, may have a considerable effect on global fires throughout history. It is therefore imperative to further improve our understanding of the human influence on fires.

[36] Using input from GISS GCM historical climate simulations, we have modeled interannual variations of global fire activity over the 1981–2000 period, and compared them to the 20-year AVHRR-based estimates [Riano *et al.*, 2007]. The model reasonably reproduces the AVHRR variability and successfully captures the large deviations

that followed the El Chichon and Pinatubo eruptions. This suggests that although the model is highly simplified, it captures many of the key physical processes that govern the response of fire to climate variations.

[37] The fire parameterization suggested in this work allows a relatively simple, yet effective and physically based representation of fire activity on a global scale. In conjunction with climate models (potentially including dynamic vegetation components), the fire parameterization offers the possibility of estimating long-term variations in global fire activity in the past and assessing possible changes in the occurrence of fires due to changing future climate.

[38] **Acknowledgments.** Our sincere thanks are due to David Riaño for kindly sharing with us the AVHRR burnt area estimates. We thank NASA's Atmospheric Chemistry Modeling and Analysis Program for supporting this work.

References

- Adler, R. F., *et al.* (2003), The version 2 Global Precipitation Climatology Project (GPCP) monthly precipitation analysis (1979-present), *J. Hydro-meteorol.*, *4*, 1147–1167, doi:10.1175/1525-7541(2003)004<1147:TVGPCP>2.0.CO;2.
- Anderson, D. B. (1939), Relative humidity or vapor pressure deficit, *Ecology*, *17*(2), 277–282, doi:10.2307/1931468.
- Arora, V. K., and G. J. Boer (2005), Fire as an interactive component of dynamic vegetation models, *J. Geophys. Res.*, *110*, G02008, doi:10.1029/2005JG000042.
- Castellvi, F., P. J. Perez, J. M. Villar, and J. I. Rosell (1996), Analysis of methods for estimating vapor pressure deficits and relative humidity, *Agric. For. Meteorol.*, *82*(1), 29–45, doi:10.1016/0168-1923(96)02343-X.
- Center for International Earth Science Information Network (CIESIN) (2005), Gridded population of the world version 3 (GPWv3): Population density grids, Palisades, NY, Socioecon. Data and Appl. Cent. (SEDAC), Columbia Univ., New York. (Available at <http://sedac.ciesin.columbia.edu/gpw>)
- Christian, H. J., K. T. Driscoll, S. J. Goodman, R. J. Blakeslee, D. A. Mach, and D. E. Buechler (1996), The Optical Transient Detector (OTD), paper presented at the 10th International Conference on Atmospheric Electricity, Osaka, Japan, June.
- Chuveico, E., L. Giglio, and C. Justice (2008), Global characterization of fire activity: Toward defining fire regimes from Earth observation data, *Global Change Biol.*, *14*, 1488–1502, doi:10.1111/j.1365-2486.2008.01585.x.
- Dale, V. H., *et al.* (2001), Climate change and forest disturbances, *BioScience*, *51*(9), 723–734, doi:10.1641/0006-3568(2001)051[0723:CCAFD]2.0.CO;2.
- Dienes, L. (2004), Observations on the problematic potential of Russian oil and the complexities of Siberia, *Eurasian Geogr. Econ.*, *45*(5), 319–345, doi:10.2747/1538-7216.45.5.319.
- Flannigan, M. D., B. D. Amiro, K. A. Logan, B. J. Stocks, and B. M. Wotton (2005a), Forest fires and climate change in the 21st century, *Mitig. Adapt. Strategies Glob. Change*, *1*, 847–859, doi:10.1007/s11027-005-9020-7.
- Flannigan, M. D., K. A. Logan, B. D. Amiro, W. R. Skinner, and B. J. Stocks (2005b), Future area burned in Canada, *Clim. Change*, *72*, 1–16, doi:10.1007/s10584-005-5935-y.
- Foley, J. A., C. Monfreda, N. Ramankutty, and D. Zaks (2007), Our share of the planetary pie, *Proc. Natl. Acad. Sci. U. S. A.*, *104*(31), 12,585–12,586, doi:10.1073/pnas.0705190104.
- Garrigues, S., *et al.* (2008), Validation and intercomparison of global Leaf Area Index products derived from remote sensing data, *J. Geophys. Res.*, *113*, G02028, doi:10.1029/2007JG000635.
- Giglio, L., J. D. Kendall, and R. Mack (2003), A multi-year fire data set for the tropics derived from the TRMM VIRS, *Int. J. Remote Sens.*, *24*(22), 4505–4525, doi:10.1080/0143116031000070283.
- Giglio, L., G. R. van der Werf, J. T. Randerson, G. J. Collatz, and P. Kasibhatla (2006), Global estimation of burned area using MODIS active fire observations, *Atmos. Chem. Phys.*, *6*, 957–974.
- Goff, J. A. (1957), Saturation pressure of water on the new Kelvin temperature scale, in *Transactions of the American Society of Heating and Ventilating Engineers, 63rd Semi-Annual Meeting*, pp. 347–354, Am. Soc. of Heating and Ventilating Eng., Murray Bay, Quebec, Canada.

- Goff, J. A., and S. Gratch (1946), Low-pressure properties of water from -160 to 212°F , in *Transactions of the American Society of Heating and Ventilating Engineers*, 52nd Annual Meeting, pp. 95–122, Am. Soc. of Heating and Ventilating Eng., New York.
- Groisman, P. Y., et al. (2007), Potential forest fire danger over Northern Eurasia: Changes during the 20th century, *Global Planet. Change*, 56, 371–386, doi:10.1016/j.gloplacha.2006.07.029.
- Guyette, R. P., R. M. Muzika, and D. C. Dey (2002), Dynamics of an anthropogenic fire regime, *Ecosystems*, 5, 472–486, doi:10.1007/s10021-002-0115-7.
- Hansen, J., et al. (2007), Climate simulations for 1880–2003 with GISS modelE, *Clim. Dyn.*, 29, 661–696, doi:10.1007/s00382-007-0255-8.
- Kalnay, E., et al. (1996), The NCEP/NCAR 40-year reanalysis project, *Bull. Am. Meteorol. Soc.*, 77, 437–471, doi:10.1175/1520-0477(1996)077<0437:TNYRP>2.0.CO;2.
- Kasischke, E. S., J. H. Hewson, B. Stocks, G. van der Werf, and J. Randerson (2003), The use of ATSR active fire counts for estimating relative patterns of biomass burning—a study from the boreal forest region, *Geophys. Res. Lett.*, 30(18), 1969, doi:10.1029/2003GL017859.
- Keetch, J. J., and G. M. Byram (1968), A drought index for forest fire control, *Res. Pap. SE-38*, For. Serv., Southeast. For. Exp. Stn., U.S. Dep. of Agric., Asheville, N. C.
- Leptoukh, G., I. Csiszar, P. Romanov, S. Shen, T. Loboda, and I. Gerasimov (2007), NASA NEESPI Data and Services Center for Satellite Remote Sensing Information, *Environ. Res. Lett.*, 2, 045009–045015, doi:10.1088/1748-9326/2/4/045009.
- Martell, D. L., E. Bevilacqua, and B. J. Stocks (1989), Modelling seasonal variation in daily people-caused fire occurrence, *Can. J. For. Res.*, 19, 1555–1563, doi:10.1139/x89-237.
- Martinez, J., E. Chuvieco, and P. Martin (2008), Estimation of risk factors of human ignition of fires in Spain by means of logistic regression, in *Proceedings of the Second International Symposium on Fire Economics, Planning, and Policy: A Global View*, Gen. Tech. Rep. PSW-GTR-208, pp. 265–278, U.S. For. Serv., Albany, Calif.
- Mollicone, D., H. D. Eva, and F. Achard (2006), Ecology: Human role in Russian wild fires, *Nature*, 440, 436–437, doi:10.1038/440436a.
- Mouillot, F., and C. H. Field (2005), Fire history and the global carbon budget: A $1^{\circ} \times 1^{\circ}$ fire history reconstruction for the 20th century, *Global Change Biol.*, 11, 398–420, doi:10.1111/j.1365-2486.2005.00920.x.
- Nesterov, V. G. (1949), *Flammability of the Forest and Methods for Its Determination (Gorimost lesa i metodi eio opredelenia)* (in Russian), Goslesbumizdat, USSR State Ind. Press, Moscow.
- Noble, I. R., G. A. V. Bary, and A. M. Gill (1980), McArthur's fire-danger meters expressed as equations, *Aust. J. Ecol.*, 5, 201–203, doi:10.1111/j.1442-9993.1980.tb01243.x.
- Prentice, S. A., and D. Mackerras (1977), The ratio of cloud to cloud-ground lightning flashes in thunderstorms, *J. Appl. Meteorol.*, 16, 545–550.
- Price, C. D. R. (1994), The impact of a $2 \times \text{CO}_2$ climate on lightning-caused fires, *J. Clim.*, 7, 1484–1494, doi:10.1175/1520-0442(1994)007<1484:TIOACC>2.0.CO;2.
- Riano, D., J. A. Moreno Ruiz, D. Isidoro, and S. L. Ustin (2007), Global spatial patterns and temporal trends of burned area between 1981 and 2000 using NOAA-NASA Pathfinder, *Global Change Biol.*, 13, 40–50, doi:10.1111/j.1365-2486.2006.01268.x.
- Saugier, B., A. Granier, J. Y. Pontailler, E. Dufrene, and D. D. Baldocchi (1997), Transpiration of a boreal pine forest measured by branch bag, sap flow and micrometeorological methods, *Tree Physiol.*, 17, 511–519.
- Schiermeier, Q. (2005), Climate change: That sinking feeling, *Nature*, 435, 732–733, doi:10.1038/435732a.
- Soja, A. J., N. M. Tchepakova, N. H. F. French, M. D. Flannigan, H. H. Shugart, B. J. Stocks, A. I. Sukhinin, E. I. Parfenova, S. F. Chapin III, and P. W. Stackhouse Jr. (2007), Climate-induced boreal forest change: Predictions versus current observations, *Global Planet. Change*, 56, 274–296, doi:10.1016/j.gloplacha.2006.07.028.
- Tanse, K., et al. (2007), L3JRC—A global, multi-year (2000–2007) burnt area product (1 km resolution and daily time steps), paper presented at Remote Sensing and Photogrammetry Society Annual Conference, Newcastle upon Tyne, U. K., Sept.
- Telitsyn, H. P. (1988), *Lesnye pozhary; ih preduprezhdenie i bor'ba s nimi v Khabarovskom Krae*, Dalnilkh, Khabarovsk.
- Thonicke, K., S. Venevsky, S. Stich, and W. Cramer (2001), The role of fire disturbance for global vegetation dynamics: Coupling fire into a dynamic global vegetation model, *Glob. Ecol. Biogeogr.*, 10, 661–677, doi:10.1046/j.1466-822x.2001.00175.x.
- Tucker, C. J., H. E. Dregne, and W. W. Newcomb (1991), Expansion and contraction of the Sahara Desert from 1980 to 1990, *Science*, 253(5017), 299–300s, doi:10.1126/science.253.5017.299.
- Van der Werf, G. R., J. T. Randerson, G. J. Collatz, and L. Giglio (2003), Carbon emissions from fires in tropical and subtropical ecosystems, *Global Change Biol.*, 9, 547–562, doi:10.1046/j.1365-2486.2003.00604.x.
- Van der Werf, G. R., J. T. Randerson, L. Giglio, G. J. Collatz, P. S. Kasibhatla, and A. F. Arellano Jr. (2006), Interannual variability in global biomass burning emissions from 1997 to 2004, *Atmos. Chem. Phys.*, 6, 3423–3441.
- Van Wagner, C. E. (1987), Development and structure of the Canadian forest fire weather index system, *For. Tech. Rep.* 35, Can. For. Serv., Ottawa, Ont., Canada.
- Venevsky, S., K. Thonicke, S. Stich, and W. Cramer (2002), Simulating fire regimes in human-dominated ecosystems: Iberian Peninsula case study, *Global Change Biol.*, 8, 984–998, doi:10.1046/j.1365-2486.2002.00528.x.
- Wotton, B. M., D. L. Martell, and K. A. Logan (2003), Climate change and people-caused forest fire occurrence in Ontario, *Clim. Change*, 60, 275–295, doi:10.1023/A:1026075919710.
- Zhdanko, V. A. (1965), Scientific basis of development of regional scales and their importance for forest fire management, in *Contemporary Problems of Forest Protection From Fire and Firefighting* (in Russian), edited by I. S. Melekhov, pp. 53–86, Lesnaya Promyshlennost, Moscow.

O. Pechony and D. T. Shindell, NASA Goddard Institute for Space Studies, Columbia University, New York, NY 10025, USA. (pechony@gmail.com)